LC-TH-2001-011

Pair Production of Smuons Near the Threshold in e^+e^- Collisions

A. Freitas, D.J. Miller and P.M. Zerwas

Deutsches Elektronen–Synchrotron DESY, D–22603 Hamburg, Germany

Abstract

Non-zero width effects are analyzed for the pair production of smuons near the threshold in e^+e^- collisions. The excitation curves are predicted in a gauge-invariant form. Energy cuts are designed to reduce irreducible supersymmetric backgrounds.

1. In supersymmetric theories [1], scalar leptons are of particular interest. Their properties can be determined with very high experimental precision in e^+e^- experiments [2, 3], which provides the platform for reconstructing the fundamental supersymmetric theory at energies up to near the Planck scale [4].

The supersymmetric partners of the left- and right-chiral leptons are the scalar leptons, $\tilde{l}_L$ and $\tilde{l}_R$. Neglecting mixing effects in the first and second family[1], the chiral states are identified with the mass eigenstates.

Scalar muons are produced pairwise in e^+e^- annihilation via s-channel photon and Z boson exchange [5]:

$$e^+e^- \to \tilde{\mu}_i^+\tilde{\mu}_i^- \quad (i = \mathrm{L/R}) \tag{1}$$

The cross section rises near the threshold $\sim \beta^3$ as a P-wave process $[\beta = (1 - 4m^2_{\tilde{\mu}_i}/s)^{\frac{1}{2}}$ denoting the smuon velocity], while becoming scale invariant for large centre-of-mass energies $\sqrt{s}$. In detail, the cross-section for the production of on-shell smuons is given by,

$$\begin{aligned} \sigma[e^+e^- \to \tilde{\mu}_i^+\tilde{\mu}_i^-] = \; & \frac{\pi\alpha^2}{3s}\left(1 - \frac{4m^2_{\tilde{\mu}_i}}{s}\right)^{\frac{3}{2}}\left[1 - g_i\,\frac{1-4s^2_{\mathrm{W}}}{s_{\mathrm{W}}c_{\mathrm{W}}}\,\frac{s}{s-M^2_{\mathrm{Z}}}\right. \\ & \left. + g_i^2\,\frac{1+(1-4s^2_{\mathrm{W}})^2}{16s^2_{\mathrm{W}}c^2_{\mathrm{W}}}\left(\frac{s}{s-M^2_{\mathrm{Z}}}\right)^2\right]. \end{aligned} \tag{2}$$

The masses are denoted by $m_{\tilde{\mu}_i}$ $(i = \mathrm{L/R})$ for the partners of the left- and right-chiral muon states; s_{W} and c_{W} are the sine and cosine of the electroweak mixing angle, and the couplings $g_{\mathrm{L}} = (-1 + 2s^2_{\mathrm{W}})/4s_{\mathrm{W}}c_{\mathrm{W}}$ and $g_{\mathrm{R}} = s_{\mathrm{W}}/c_{\mathrm{W}}$ denote the Z charges of the L/R smuons. The fine structure constant α is evaluated at the scale $\sqrt{s}$.

The right-chiral smuons decay predominantly into neutralinos while additional chargino decays are also important for left-chiral smuons [6]:

$$\Gamma(\tilde{\mu}_i^- \to \mu^-\tilde{\chi}^0_j) \;=\; \alpha|X_{ij}|^2\, m_{\tilde{\mu}_i}\left(1 - \frac{m^2_{\tilde{\chi}^0_j}}{m^2_{\tilde{\mu}_i}}\right)^2, \tag{3}$$

$$\Gamma(\tilde{\mu}_{\mathrm{L}}^- \to \nu_\mu\tilde{\chi}^-_k) \;=\; \frac{\alpha}{4}|U_{k1}|^2 m_{\tilde{\mu}_{\mathrm{L}}}\left(1 - \frac{m^2_{\tilde{\chi}^-_k}}{m^2_{\tilde{\mu}_{\mathrm{L}}}}\right)^2, \tag{4}$$

where

$$X_{ij} = \frac{1}{\sqrt{2}}(N'_{j1} - g_i N'_{j2}), \tag{5}$$

[1]Mixing effects in the smuon sector are of the order 10^{-5} and can be safely neglected, provided the left- and right-chiral sleptons are well separated in mass.

with $m_{\tilde{\chi}_j^0}$ $(j = 1, ..., 4)$ denoting the four neutralino masses, and $m_{\tilde{\chi}_k^\pm}$ $(k = 1, 2)$ the two chargino masses in the minimal supersymmetric extension of the Standard Model. The neutralino mixing matrix N' relates the mass eigenstates with the eigenstates in the photino-Zino-Higgsino basis, and U is the corresponding mixing matrix for the negative charginos. For a right-chiral smuon mass in the range of about 200 GeV, the width, suppressed relative to the mass by the coupling α, is of the order $\Gamma_{\tilde{\mu}_{\rm R}} \sim 700$ MeV.

2. The measurement of the smuon excitation curve near the threshold is the most accurate method of determining the masses. Detailed simulations have demonstrated that the right-chiral smuon mass can be measured at TESLA to an accuracy of less than 100 MeV in this way [3], *i.e.* a fraction of a per-mille. This experimental error is significantly smaller than the width of the state. Therefore, in this report we examine the effect of non-zero smuon widths on the excitation curves. Additionally, an accurate theoretical prediction requires the calculation of higher order effects, notably multiple photon exchange among the final state particles. The problems arising in this context are quite similar to the production of W pairs in e^+e^- annihilations [7]. The calculation of these higher order effects will be described in a subsequent report. Moreover, for the sake of clarity we will restrict ourselves to the analysis of right-chiral smuons.

Decays of the right-chiral smuons to the LSP $\tilde{\chi}_1^0$,

$$\tilde{\mu}_R^- \to \mu^- \tilde{\chi}_1^0, \tag{6}$$

are by far the dominant decay mode in the Minimal Supersymmetric Standard Model (MSSM). The parameters, masses and couplings, we have adopted for illustrative examples, correspond to the large $\tan\beta$ reference point **RR2** in the TESLA study Ref. [8]. The relevant physical parameters are summarized in the appendix. The pair production of off-shell smuons is described in this final state by the diagram Fig.(1a):

$$e^+e^- \to \mu^+\mu^-\tilde{\chi}_1^0\tilde{\chi}_1^0. \tag{7}$$

However, the double resonance diagram must be supplemented by the single resonance diagrams of Fig.(1b) to generate a gauge invariant set for the off-shell production amplitude.

If the $[\mu\tilde{\chi}_1^0]$ final states are studied near the $\tilde{\mu}$ mass, the real $\tilde{\mu}$ propagators must be replaced by the Breit-Wigner form which explicitly includes the non-zero width of the

(a) Double resonance diagram

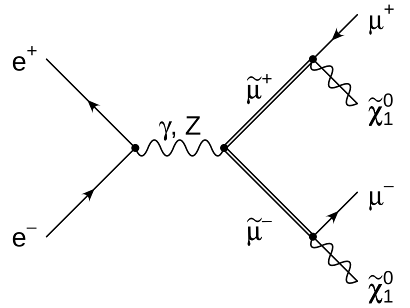

(b) Single resonance diagrams

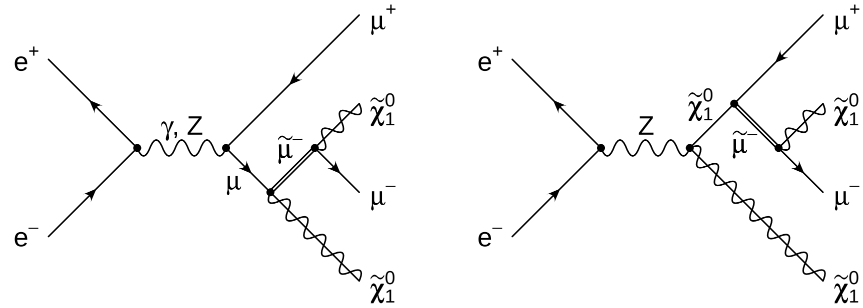

Figure 1: *The doubly and singly resonant contributions to the process* $e^+e^- \to \mu^+\mu^-\tilde{\chi}^0_1\tilde{\chi}^0_1$.

resonance state. Near the threshold the substitution leaves the set of diagrams Fig.(1) gauge invariant if the complex mass

$$m^2_{\tilde{\mu}} \to m^2_{\tilde{\mu}} - i m_{\tilde{\mu}} \Gamma_{\tilde{\mu}} \tag{8}$$

is introduced with fixed width $\Gamma_{\tilde{\mu}}$. Applying the substitution to the propagators in the double and single resonance amplitudes provides a consistent scheme for smuon production near the thresholds. Even though taking only the doubly resonant contribution Fig.(1a) with fixed width in the covariant gauge (a scheme generally adopted for experimental simulations [3]) is of sufficient accuracy at high energies, it fails for high-precision analyses near the threshold. Indeed the error induced by this method, about 80 MeV, is generally of the same size as the error of the experimental measurement.

The effect of non-zero width $\Gamma_{\tilde{\mu}_R}$ on the $\tilde{\mu}^+_R\tilde{\mu}^-_R$ excitation curve near the threshold is demonstrated in Fig.(2) for the **RR2** parameters. While the excitation curve is shown for zero width by the dotted line, the prediction of the excitation curve including the non-zero width effect in a gauge-invariant form is shown by the full line which can be

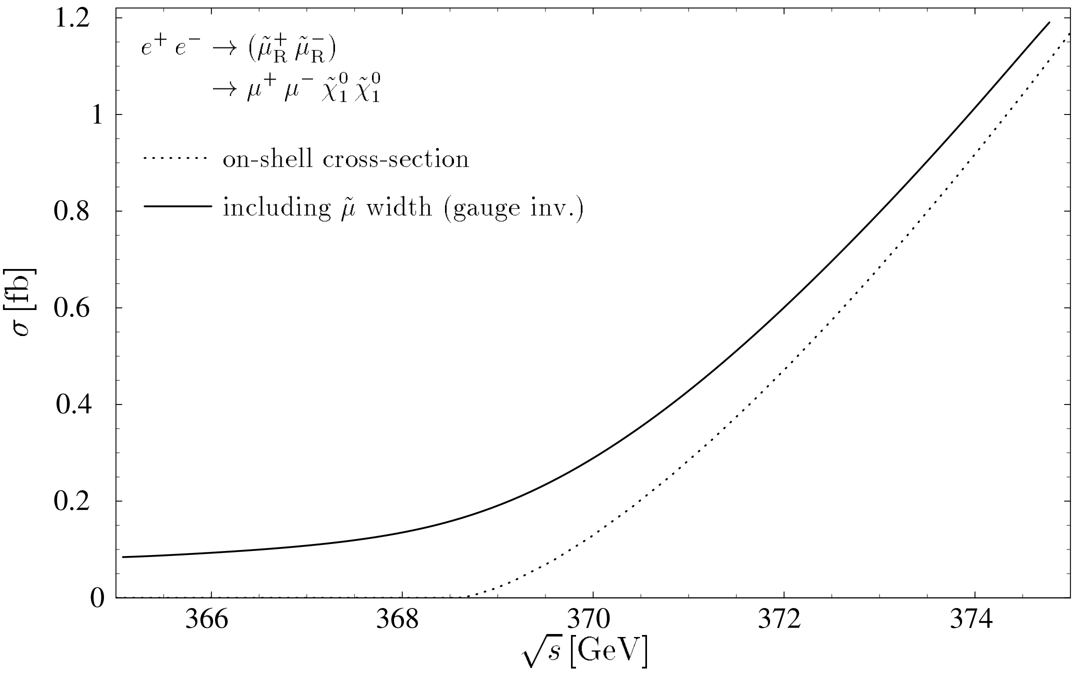

Figure 2: *The effect of finite $\tilde{\mu}$ width on the $e^+e^- \to \tilde{\mu}_R^+\tilde{\mu}_R^- \to \mu^+\mu^-\tilde{\chi}_1^0\tilde{\chi}_1^0$ cross-section.*

interpreted as the "signal cross-section".

3. A large number of SUSY backgrounds contribute to the smuon signal in the process $e^+e^- \to \mu^+\mu^- + \not{E}$. Classes of background processes are catalogued in Tab.(1). The most important cross-sections are shown in Fig.(3a). The background processes can be reduced to a controllable level by applying cuts on the muon energies and on the missing energy.

(i) Background processes involve decay cascades which give rise to threshold effects in the muon-pair invariant mass and increased missing energy compared to the signal process. The large $\tilde{\chi}_2^0\tilde{\chi}_1^0$ background can be reduced drastically by selecting events with invariant mass

$$m_{\mu\mu} \gtrsim m_{\tilde{\chi}_2^0} - m_{\tilde{\chi}_1^0} \tag{9}$$

which amounts to 60 GeV for the mass values of the reference point. In addition, requiring

(a)

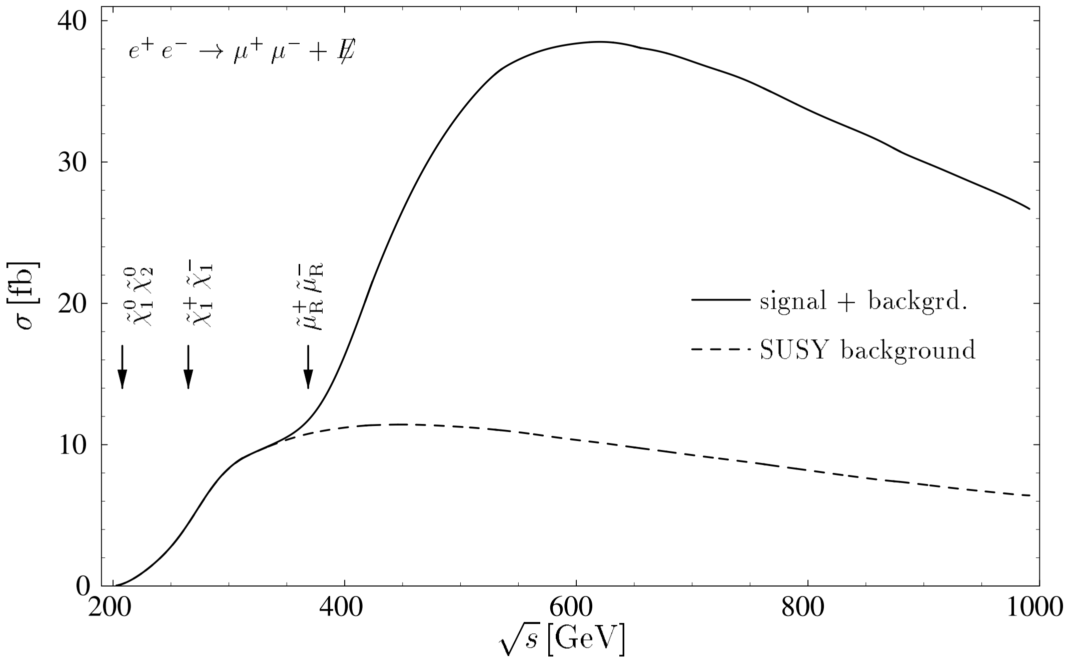

(b)

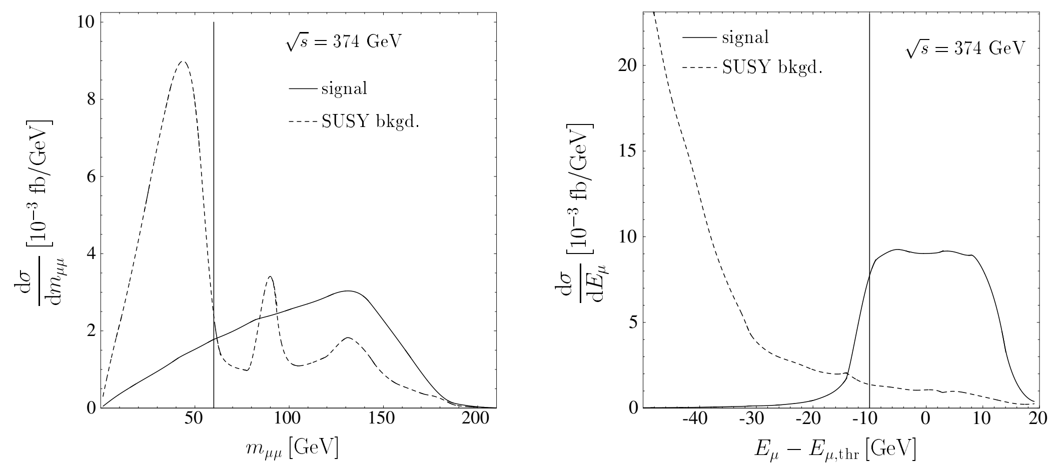

Figure 3: *(a) The total cross-section and SUSY backgrounds to* $e^+e^- \to \mu^+\mu^- + \not{E}$*, indicating the important nominal thresholds by arrows. (b) The distributions in the muon-pair invariant mass (after the missing energy cut has been made) and muon energy, with possible cuts shown as a solid vertical line.*

Source Process	Followed by	
$e^+e^- \to \tilde{\chi}^0_k\tilde{\chi}^0_1$	$\tilde{\chi}^0_k \to \mu^+\mu^-\tilde{\chi}^0_1$	
$e^+e^- \to \tilde{\chi}^0_2\tilde{\chi}^0_2$	$\tilde{\chi}^0_2 \to \mu^+\mu^-\tilde{\chi}^0_1$	$\tilde{\chi}^0_2 \to \bar{\nu}\nu\tilde{\chi}^0_1$
$e^+e^- \to \tilde{\chi}^+_1\tilde{\chi}^-_1$	$\tilde{\chi}^\pm_1 \to \mu^\pm\nu_\mu\tilde{\chi}^0_1$	
$e^+e^- \to ZZ$	$Z \to \mu^+\mu^-$	$Z \to \tilde{\chi}^0_1\tilde{\chi}^0_1$
$e^+e^- \to Z\, h_0/H_0$	$Z \to \mu^+\mu^-$	$h_0/H_0 \to \tilde{\chi}^0_1\tilde{\chi}^0_1$

Table 1: *The significant doubly-resonant SUSY background processes contributing to* $e^+e^- \to \mu^+\mu^- + \not{E}$ *near the* $\tilde{\mu}^+_{\rm R}\tilde{\mu}^-_{\rm R}$ *production threshold. Singly-resonant and non-resonant SUSY backgrounds are also included in the analysis.*

the missing energy $\not{E}$ below the cut

$$\not{E} \lesssim E_{\rm cut} = \sqrt{s} - \frac{(m^2_{\tilde{\chi}^0_2} - m^2_{\tilde{\chi}^0_1})\left(s - m^2_{\tilde{\chi}^0_1} + m^2_{\tilde{\chi}^0_2} - \lambda^{1/2}(s, m^2_{\tilde{\chi}^0_1}, m^2_{\tilde{\chi}^0_2})\right)}{4\sqrt{s}\, m^2_{\tilde{\chi}^0_2}} \tag{10}$$

eliminates a large fraction of the background events from $\tilde{\chi}^0_1\tilde{\chi}^0_2$ cascades to $\mu^+\mu^-\tilde{\chi}^0_1\tilde{\chi}^0_1$. In the scenario **RR2**, events with missing energy below a fraction 0.63 of the c.m. energy are kept in the signal sample. Only a small number of signal events are lost while the $\tilde{\chi}^0_1\tilde{\chi}^0_2$ background is reduced by a factor of fifty. After applying these two cuts we are left with a small amount of higher cascade decays. This is apparent from Fig.(3b/left) which shows the invariant μ-pair mass after the missing energy cut has already been applied.

(ii) Near the threshold the observed muon energy is sharp:

$$E_\mu \approx (m^2_{\tilde{\mu}} - m^2_{\tilde{\chi}^0_1})/2m_{\tilde{\mu}} \tag{11}$$

Alternatively to the $\not{E}$ cut, the signal to background ratio can be greatly enhanced by selecting muons with energies in a band $\delta E \approx 10$ GeV about the nominal threshold energies, cf. Fig.(3b/right).

Additional cuts, familiar from SM background studies [3], are necessary to avoid the detector regions near the beam pipe, *i.e.* $|\cos\theta_\mu| < 0.95$ and $|\cos\theta_{\not{p}}| < 0.9$. These cuts have a small effect on the SUSY induced signals and backgrounds, as have other SM motivated cuts [3], and are not included in this analysis.

The matrix elements were calculated using the computer algebra package *FeynArts* [9]. Due to the large number of diagrams involved, it was convenient to perform the evaluation in terms of helicity amplitudes which were then evaluated using the Dirac spinor techniques of Ref. [10]. The phase-space integration was performed by multi-channel Monte-Carlo methods where appropriate phase-space mappings were used in order to obtain numerically stable results of high accuracy [11]. The Monte-Carlo error was reduced by adaptive weight optimization [12]. Initial state radiation from emission of collinear and soft photons is included using the structure-function method [13] up to second order in the leading-log approximation and soft-photon exponentiation [14]. Beamstrahlung effects are also included using the program $K\iota\rho\kappa\eta$ [15] for TESLA accelerator design parameters.

4. Including the SUSY backgrounds, the excitation curves, after the beamstrahlung is switched on and the cuts are applied, are shown in Fig.(4a & b). As evident from the two figures, the background is smooth below the signal curve in the threshold region. The background can therefore be extrapolated from below into the threshold region and subtracted experimentally in a model-independent way since interference effects are small.

In summary, the present report describes a first theoretical step into the area of high-precision analyses in supersymmetric theories. We have concentrated on non-zero width effects in the threshold production of smuon pairs. It is evident that many additional detailed calculations must follow to reach final theoretical accuracies at a level of a per-mille as required by the expected accuracy in TESLA analyses.

Acknowledgments

We are grateful to H. U. Martyn for useful discussions.

(a)

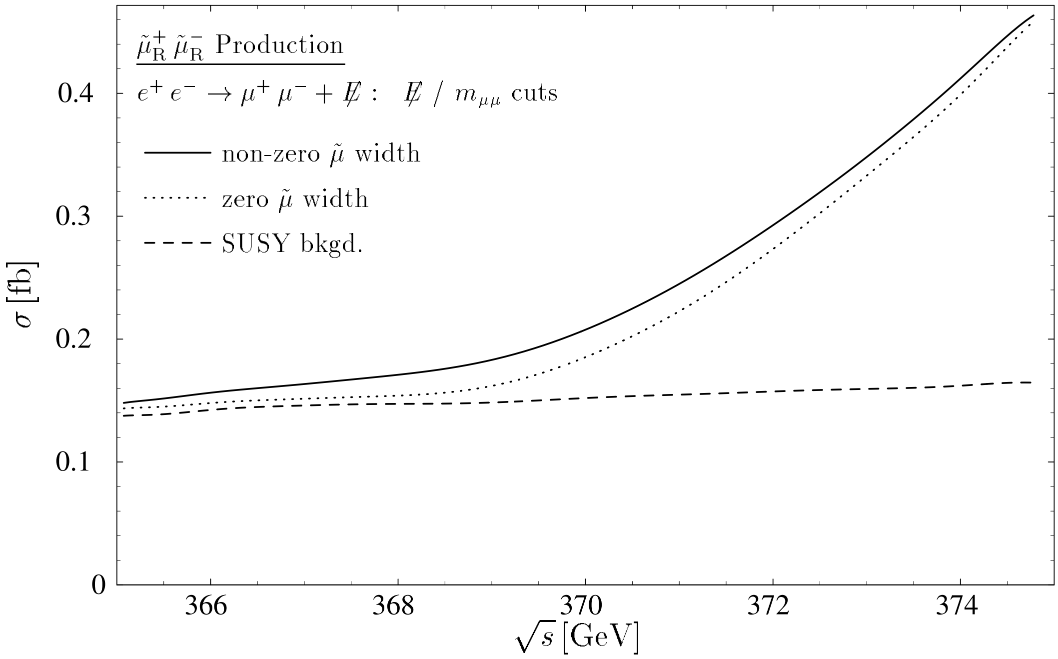

(b)

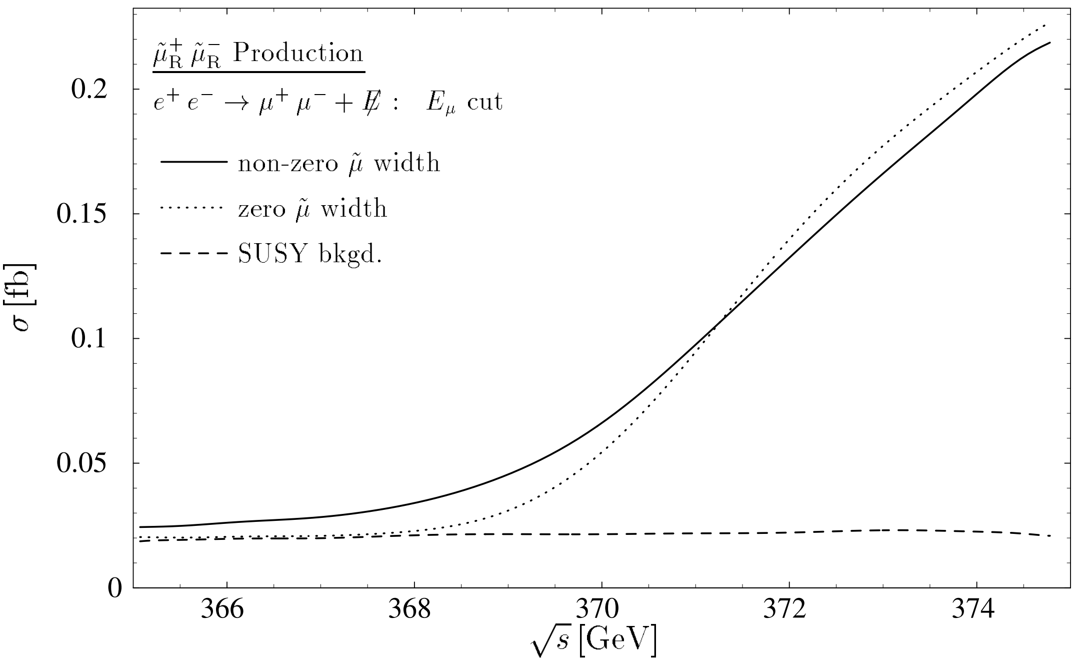

Figure 4: *The excitation curves for the signal (with non-zero and zero width) and the SUSY background after (a) the missing energy cut and, alternatively, (b) the muon energy cut.*

Appendix

Reference scenario **RR2** with $\tan\beta = 30$:

Neutralino masses:

	$m_{\tilde{\chi}_i^0}$ [GeV]
$\tilde{\chi}_1^0$	74.81
$\tilde{\chi}_2^0$	133.04
$\tilde{\chi}_3^0$	272.81
$\tilde{\chi}_4^0$	292.96

Chargino masses:

	$m_{\tilde{\chi}_i^\pm}$ [GeV]
$\tilde{\chi}_1^\pm$	132.35
$\tilde{\chi}_2^\pm$	294.84

Right-chiral smuon $\tilde{\mu}_{\rm R}$:

Mass $m_{\tilde{\mu}}$	184.29 GeV
Width $\Gamma_{\tilde{\mu}}$	0.62 GeV

Branching Ratios	
$\tilde{\mu}_{\rm R}^- \to \mu^- \, \tilde{\chi}_1^0$	0.991
$\to \mu^- \, \tilde{\chi}_2^0$	0.008
$\to \mu^- \, \tilde{\chi}_{3,4}^0$	—

Left-chiral smuon $\tilde{\mu}_{\rm L}$:

Mass $m_{\tilde{\mu}}$	217.19 GeV
Width $\Gamma_{\tilde{\mu}}$	1.03 GeV

Branching Ratios	
$\tilde{\mu}_{\rm L}^- \to \mu^- \, \tilde{\chi}_1^0$	0.144
$\to \mu^- \, \tilde{\chi}_2^0$	0.338
$\to \mu^- \, \tilde{\chi}_{3,4}^0$	—
$\to \nu_\mu \, \tilde{\chi}_1^-$	0.517
$\to \nu_\mu \, \tilde{\chi}_2^-$	—

References

[1] J. Wess and B. Zumino, Nucl. Phys. B **70** (1974) 39; Phys. Lett. B **49** (1974) 52.

[2] E. Accomando et al, Phys. Rept. **299** (1998) 1.

[3] H. U. Martyn and G. A. Blair, Proceedings, *4th International Workshop on Linear Colliders* (LCWS 99), Sitges 1999, [hep-ph/9910416]; H. U. Martyn, Workshop on Physics at TeV Colliders, Les Houches 1999, [hep-ph/0002290].

[4] G. A. Blair, W. Porod and P. M. Zerwas, Phys. Rev. D **63** (2001) 017703.

[5] M. K. Gaillard, L. Hall and I. Hinchliffe, Phys. Lett. B **116** (1982) 279; M. Glück and E. Reya, Phys. Lett. B **130** (1983) 423; R. M. Barnett, H. E. Haber and K. S. Lackner, Phys. Rev. D **29** (1984) 1381; D. H. Schiller and D. Wahner, Nucl. Phys. B **255** (1985) 505; T. Kobayashi and M. Kuroda, Phys. Lett. B **134** (1984) 271;

[6] T. Schimert and X. Tata, Phys. Rev. D **32** (1985) 721; A. Bartl, H. Fraas and W. Majerotto, Z. Phys. C **34** (1987) 411; T. Tsukamoto, K. Fujii, H. Murayama, M. Yamaguchi and Y. Okada, Phys. Rev. D **51** (1995) 3153; B. de Carlos and M. A. Diaz, Phys. Lett. B **417** (1998) 72.

[7] See *e.g.*, V. S. Fadin, V. A. Khoze, A. D. Martin and A. Chapovsky, Phys. Rev. D **52** (1995) 1377; A. Denner, S. Dittmaier, M. Roth and D. Wackeroth, Nucl. Phys. B **560** (1999) 33.

[8] See, S. Ambrosanio, G. A. Blair, P. M. Zerwas, *A Study of* SUGRA *for the Linear Collider*, [`http://www.hep.ph.rhbnc.ac.uk/~blair/susy`].

[9] J. Küblbeck, M. Böhm, A. Denner, Comput. Phys. Commun. **60** (1991) 165; T. Hahn, *FeynArts 2.2 User's Guide*, [`http://www.ferynarts.de/`]; A. Denner, H. Eck, O. Hahn and J. Küblbeck, Nucl. Phys. B **387** (1992) 467; T. Hahn, Nucl. Phys. Proc. Suppl. **89** (2000) 231; A. Kraft, Ph.D. Thesis (University of Karlsruhe 1999); T. Hahn, hep-ph/0007062.

[10] R. Kleiss and W. J. Stirling, Nucl. Phys. B **262** (1985) 235.

[11] F. A. Berends, P. H. Daverveldt and R. Kleiss, Nucl. Phys. B **253** (1985) 441 and Comput. Phys. Commun. **40** (1986) 285; J. Hilgart, R. Kleiss and F. Le Diberder, Comput. Phys. Commun. **75** (1993) 191; F. A. Berends, R. Pittau and R. Kleiss, Nucl. Phys. B **424** (1994) 308.

[12] R. Kleiss and R. Pittau, Comput. Phys. Commun. **83** (1994) 141.

[13] E. A. Kuraev and V. S. Fadin, Sov. J. Nucl. Phys. **41** (1985) 466; G. Altarelli and G. Martinelli, in *Physics at LEP*, eds. J. Ellis, R. Peccei, CERN-86-02.

[14] D. R. Yennie, S. C. Frautschi and H. Suura, Annals Phys. **13** (1961) 379; F. A. Berends *et al*, in *Z Physics at LEP 1*, eds. G. Altarelli, R. Kleiss, C. Verzegnassi, CERN-89-08.

[15] T. Ohl, Comput. Phys. Commun. **101** (1997) 269.